Rahman, M.M.; Sadrul Islam, A.K.M.; Lampinen, M.J.; Siikonen, T.

Modified Norris-Reynolds one-equation model

Published in:
Procedia Engineering

DOI:
10.1016/j.proeng.2015.05.110

Published: 01/01/2014

Document Version
Publisher's PDF, also known as Version of record

Available online at www.sciencedirect.com

ScienceDirect

Procedia Engineering 105 (2015) 276 – 286

Procedia Engineering

www.elsevier.com/locate/procedia

6th BSME International Conference on Thermal Engineering (ICTE 2014)

Modified Norris–Reynolds One–Equation Model

M. M. Rahman[a,*], J. Taghinia[a], A.K.M. Sadrul Islam[b], M. J. Lampinen[a], T. Siikonen[a]

[a]*Aalto University School of Engineering, P.O. Box 14400, FI–00076 AALTO, Finland*
[b]*Department of Mechanical & Chemical Engineering, Islamic University of Technology, Board Bazar, Gazipur 1704, Bangladesh*

Abstract

A modified version of Norris–Reynolds (NR) k–equation turbulence model is proposed to account for the distinct effects of low–Reynolds number (LRN) and wall proximity. The turbulent kinetic energy k and the dissipation rate ϵ are evaluated using the k–transport equation in conjunction with the Bradshaw and other empirical relations. The eddy–viscosity formulation maintains the positivity of normal Reynolds stresses and preserves the anisotropic characteristics of turbulence in the sense that they are sensitized to rotational and non–equilibrium flows. The modified NR (MNR) model is validated against well–documented flow cases yielding predictions in good agreement with the direct numerical simulation (DNS) and experimental data. Comparisons indicate that the MNR model offers some improvement over the original NR model and competitiveness with the Spalart–Allmaras one–equation model.

Peer-review under responsibility of organizing committee of the 6th BSME International Conference on Thermal Engineering (ICTE 2014)

Keywords: One–equation model, turbulence anisotropy, two–layer model, non–equilibrium flow

1. Introduction

One–equation eddy–viscosity turbulence models require the input of velocity and length scales that are often obtained from the transport equation of turbulent kinetic energy k and an algebraic length scale determining quantity such as the dissipation ϵ or the specific dissipation ω. This form of transport equation is attractive due to its simplicity in implementation and much less demanding computational requirements, compared with the standard two–equation k–ϵ and k–ω models. The algebraic model such as the Baldwin–Lomax model [1] is efficient from a computational point of view but lacks generality for not having the convection and diffusion effects. However, one–equation models include the convection and diffusion effects and can be considered as a good compromise between the algebraic and two–equation models.

* Corresponding author. Tel.: +358-409626752
E-mail address: mizanur.rahman@aalto.fi

Peer-review under responsibility of organizing committee of the 6th BSME International Conference on Thermal Engineering (ICTE 2014)
doi:10.1016/j.proeng.2015.05.110

Nomenclature

a_1	turbulent structure parameter
C_f	friction coefficient
C_μ	eddy-viscosity coefficient
f_μ	eddy-viscosity damping function
h	step height
k	turbulent kinetic energy
$l_{\mu,\epsilon}$	turbulent length scales
P_k	production of turbulent kinetic energy
Re_y	turbulent Reynolds number
S	mean strain-rate invariant
T_t	hybrid time scale
t	time
u, v	velocity components in x- and y-directions
u_τ	friction velocity
$\rho\overline{u_i u_j}$	Reynolds stress tensor
W	mean vorticity invariant
x, y	Cartesian coordinates
y^+	non-dimensional normal distance from the surface
δ_{ij}	Kronecker's delta
ϵ	dissipation of turbulent kinetic energy
μ	dynamic viscosity
ν	kinematic viscosity
ρ	density
σ_k	turbulent Prandtl number
u_τ	shear stress

In principle, one–equation models have been developed in an attempt at improving turbulent flow predictions by solving an additional transport equation. While several turbulent scales have been used as the variable in the extra transport equation, the most popular method is to solve for the characteristic turbulent velocity scale proportional to the square root of specific kinetic energy k of turbulent fluctuations. The one–equation model proposed by Norris and Reynolds [2] accounted for history effects on the turbulent kinetic energy, and therefore considered an improvement over the algebraic models. However, this model still uses the same ad–hoc assumptions as with the algebraic model and most researchers have abandoned the one–equation (k–equation) model in the favor of one–equation models based on the transport equations for the eddy viscosity μ_T [3–10].

Considerable research has been devoted to improving the accuracy of one–equation μ_T models for both equilibrium and non–equilibrium flows. The Baldwin–Barth (BB) model [3] derived using the k–ϵ closure is one of the first one–equation models that does not explicitly use the algebraic length scales. It employs some assumptions that weaken its link with the k–ϵ closure; the simplification to a one–equation model is made by allowing a semi–local near–wall term. As a result, the BB model performs very differently compared to the k–ϵ model even for simple equilibrium flows [5]. However, the BB model has good near–wall properties, e.g., it has a linear behavior of the eddy–viscosity, and therefore does not require a finer grid close to the wall which is required by an algebraic model [6]. Spalart and Allmaras (SA) [4] derived their model using empiricism and arguments of dimensional analysis, having no link to the k–ϵ equations; they use the BB turbulence model as a framework for their model. The key modification made in this model is the approach to determining the semi–local near–wall term. Rahman et al. [9,10] have extended the ability

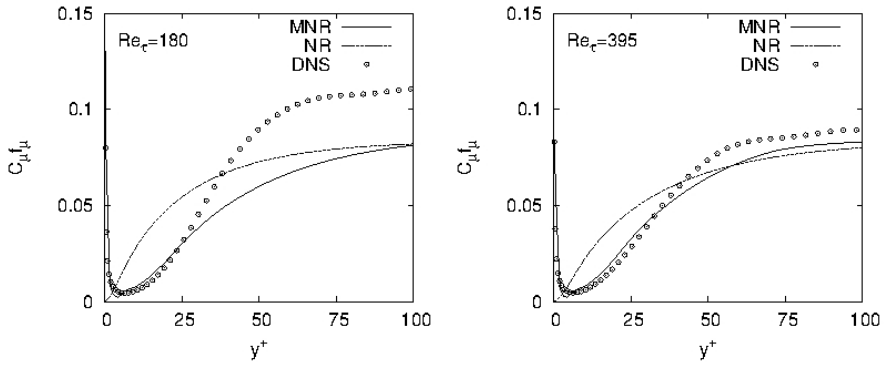

Fig. 1. Eddy–viscosity coefficients with wall distance in channel flow.

of the BB model to account for the non–equilibrium and anisotropic effects, a feature that has been missing in all the one–equation models developed to date.

In particular, the NR model is constrained by well–known shortcomings inherited from the mixing–length model. Nevertheless, this model boasts its simplicity, economy and robustness. These merits motivate the current study wherein the near–wall and low–Reynolds number (LRN) modifications to the Norris–Reynolds (NR) model are proposed and evaluated. The proposed version has several desirable attributes relative to the original NR model: (*a*) using the turbulence structure parameter $a_1 = |-\overline{uv}|/k$ (Bradshaw–relation implies that the shear stress $-\overline{uv}$ in the boundary layer is proportional to the turbulent kinetic energy k), a physically appropriate time scale is introduced that never falls below the Kolmogorov (dissipate eddy) time scale; (*b*) the eddy–viscosity coefficient C_μ depends on both the mean strain–rate and vorticity tensors; (*c*) the algebraic length–scale retains the anisotropic feature of the flow; (*d*) the eddy–viscosity damping function f_μ reproduces the asymptotic limit involving the distinct effects of LRN and wall proximity (i.e., near–wall turbulence). Consequently, the proposed modifications to the NR model extend its ability to account for the non–equilibrium and anisotropic effects, providing good results for flows with separation and reattachment.

The performance of the new model is demonstrated through the comparison with the experimental and DNS data of well–documented flows, namely the fully developed channel flows and a backward facing step flow. These test cases are selected such as to justify the ability of the modified NR model to replicate the combined effects of LRN, near–wall turbulence and non–equilibrium.

2. Norris–Reynolds (NR) model

Norris and Reynolds [2] proposed a one–equation model that shows promise as an alternative to the highly empirical–correlation dependent mixing–length model. Their intention was to develop a one–equation model that is valid right down to the wall. In collaboration with the Reynolds–averaged Naiver–Stokes (RANS) equations, the transport equation for the turbulent kinetic energy k is given by:

$$\frac{\partial \rho k}{\partial t} + \frac{\partial \rho u_j k}{\partial x_j} = \frac{\partial}{\partial x_j}\left[\left(\mu + \frac{\mu_T}{\sigma_k}\right)\frac{\partial k}{\partial x_j}\right] + \rho P_k - \rho \epsilon \tag{1}$$

where ρ is the density, μ implies the molecular viscosity, and the turbulent Prandtl number $\sigma_k(= 1.0)$ connects the diffusive of k to the eddy–viscosity. The production term $P_k = -\overline{u_i u_j}(\partial u_i/\partial x_j)$, where the Reynolds stresses $\rho\overline{u_i u_j}$ can be related to the mean strain–rate tensor S_{ij} through the Boussinesq approximation:

$$-\rho\overline{u_i u_j} = 2\mu_T\left(S_{ij} - \frac{1}{3}S_k\delta_{ij}\right) - \frac{2}{3}\rho k\delta_{ij} \tag{2}$$

where δ_{ij} is the Kronecker delta function.

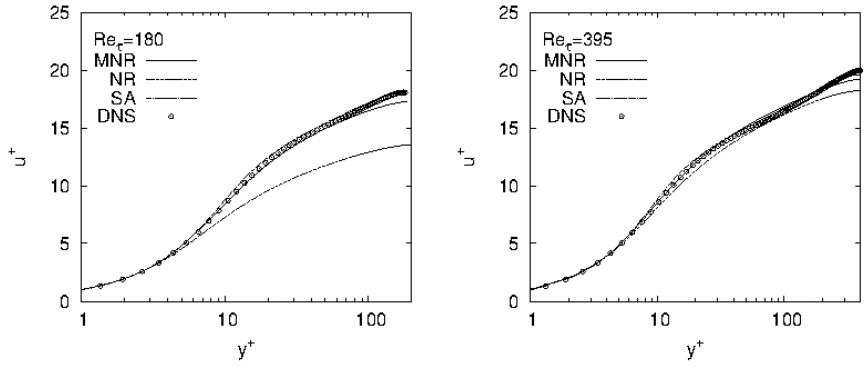

Fig. 2. Mean velocity profiles of channel flow.

With the low–Reynolds number (LRN) one–equation model, the k–equation is solved by assigning $k = 0$ on the solid boundary. Instead of solving the dissipation ϵ–equation, ϵ near the wall is determined using k and a length scale l_ϵ. The eddy–viscosity μ_T is calculated using k and a length scale l_μ, similar to ϵ:

$$\mu_T = C_\mu \rho \sqrt{k}\, l_\mu, \qquad \epsilon = \frac{k^{3/2}}{l_\epsilon} \tag{3}$$

where $C_\mu = 0.084$. The length scales l_μ and l_ϵ are proportional to the turbulent eddy–scale l ($= \kappa y$, where y denotes the distance to the wall) and are evaluated using the following relations:

$$l_\mu = C_l y \left[1 - exp\left(-\frac{Re_y}{A_\mu}\right)\right], \qquad l_\epsilon = \frac{C_l y}{1 + C_\epsilon / Re_y} \tag{4}$$

where $\kappa = 0.41$ is the von Karman constant, $Re_y = \sqrt{k} y/\nu$ denotes the turbulent Reynolds number and the kinematic viscosity $\nu = \mu/\rho$. Other model coefficients are given as $C_l = \kappa/C_\mu^{3/4}$, $A_\mu = 50.5$ and $C_\epsilon = 5.1$. In Equation (4), it is assumed that the turbulent transport is suppressed by the presence of the wall and the length scales do nothing special in the viscous region; however behave like $l = \kappa y$ right down to the wall.

One–equation models have a somewhat better history in predicting flows with separation and reattachment; however, they share most of the failures of the mixing–length model. The specification of the mixing–length by an algebraic formula is still almost entirely dependent on empirical data, and is usually incapable of including transport effects on the length scale. The desire to include transport effects on the length scale is the primary reason for introducing two–equation models such as the k–ϵ and k–ω models. In the literature, the Norris–Reynolds LRN one–equation model has been referred to as the two–layer model [11]. It is a combination of the standard k–ϵ model, used to deal with the main flow field away from the wall surface, and the NR model is applied to the near–wall region where the viscous stresses dominate. This scheme has been reported to compute transition in flows with separation and reattachment [12]. Various strategies for two–layer k–ϵ models are employed to avoid the problem with an LRN model; it requires a high grid resolution near the wall due to the steep rate of decline in ϵ toword the wall and this in turn leads to high computational costs.

Nevertheless, it is possible that one can do much better (as a single one–equation model) with the NR model in most flows of interest, for it may be easier to specify the length–scale distribution than to compute it with a partial differential equation. This would be particularly true if the length scale is really governed by an anisotropic feature of the flow. Hence, further study of an extended one–equation model based on the k–equation is encouraged.

3. Modified NR (MNR) model

An important criterion regarding the appropriateness of the turbulence model is to represent the near–wall behavior of turbulence quantities accompanied by a preferential damping of velocity fluctuations in the direction normal to the

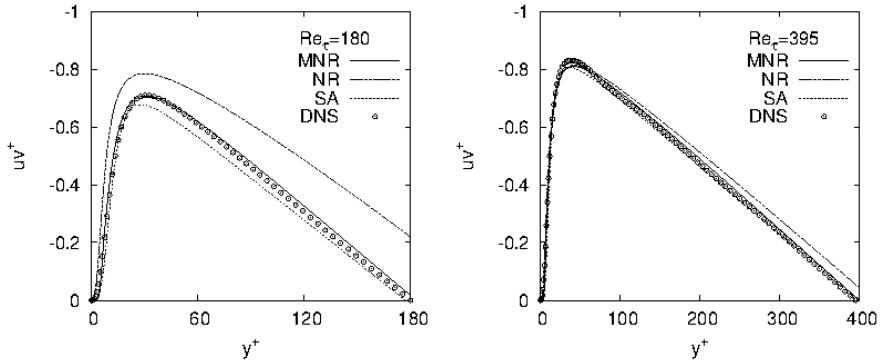

Fig. 3. Shear stress profiles of channel flow.

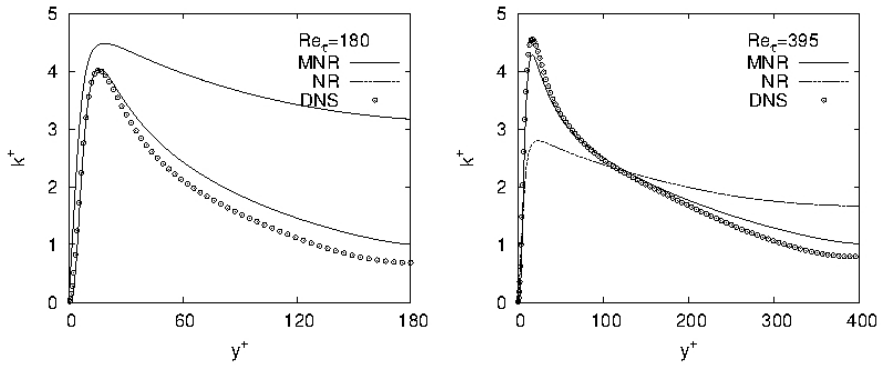

Fig. 4. Turbulence kinetic energy profiles of channel flow.

wall that reconciles the influence of wall proximity adequately. To invoke this phenomenon, the eddy viscosity μ_T is formulated as

$$\mu_T = f_\mu C_\mu \rho\, k\, T_t, \qquad C_\mu = \min\left(\tilde{C}_\mu;\, C^*_\mu f_\mu\right) \tag{5}$$

where $C^*_\mu = 0.09$ and T_t is a hybrid time scale. The coefficient $\tilde{C}_\mu$ is constructed as a scalar function of the invariants formed by the strain–rate S_{ij} and vorticity W_{ij} tensors, defined as

$$S_{ij} = \frac{1}{2}\left(\frac{\partial u_i}{\partial x_j} + \frac{\partial u_j}{\partial x_i}\right), \quad W_{ij} = \frac{1}{2}\left(\frac{\partial u_i}{\partial x_j} - \frac{\partial u_j}{\partial x_i}\right) \tag{6}$$

The invariants of mean strain–rate and vorticity tensors are given by $S = \sqrt{2S_{ij}S_{ij}}$ and $W = \sqrt{2W_{ij}W_{ij}}$, respectively. To ensure the realizability in turbulence modeling, a plausible formulation for $\tilde{C}_\mu$ as suggested in Reference [14] is adopted:

$$\tilde{C}_\mu = \frac{1}{2\left(1 + T_t S\, \sqrt{1 + \mathfrak{R}^2}\right)} \tag{7}$$

where $\mathfrak{R} = |W/S|$ is a dimensionless parameter that is very useful to characterize the flow. For instance, for a pure shear flow $\mathfrak{R} = 1$, whereas for a plane strain flow $\mathfrak{R} = 0$. It is appropriate to emphasize that the shear and vorticity parameters $T_t S$ and $T_t W$, respectively, can assist $\tilde{C}_\mu$ in responding to both the shear and vorticity dominated flows that are far from equilibrium. Detailed analysis of the model realizability is available elsewhere [15–18].

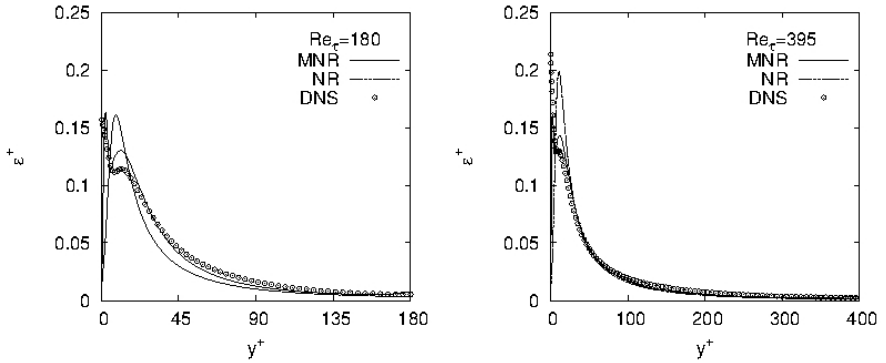

Fig. 5. Dissipation rate profiles of channel flow.

The dissipation of turbulent kinetic energy ϵ plays a vital role in determining the time scale T_t. Equations (3–4) are slightly modified to evaluate ϵ:

$$\epsilon = \frac{k^{3/2}\tilde{C}_\mu^{3/4}}{\kappa\, y}\left(1 + \frac{6}{Re_y}\right) \tag{8}$$

where $\kappa = 0.387$ is used; although a range of values for κ is available [19]. Note that unlike the original NR model, $\tilde{C}_\mu$ in the modified NR model is not a constant as given by Equation (7). On the contrary, the reduced dissipation rate $\tilde{\epsilon} \to 0$ as the wall is approached (while ϵ remains finite) can be calculated from the Bradshaw hypothesis [20], which has been implemented in many turbulence models [7]. Using the Bradshaw–relation, $\tilde{\epsilon}$ may be expressed in terms of a tentative eddy–viscosity $\tilde{\mu}_T$ via the turbulence structure parameter:

$$\frac{|-\overline{uv}|}{k} = a_1 = \frac{\tilde{\mu}_T}{\rho}\,\frac{\eta}{k} = f_\mu \tilde{C}_\mu\,\frac{\eta k}{\tilde{\epsilon}}, \qquad \eta = S\ \max(1, \Re) \tag{9}$$

where the turbulence structure parameter $a_1 = \sqrt{\tilde{C}_\mu}$. Recent DNS and experimental data indicate that this hypothesis is not exactly valid in the viscous sublayer of the turbulent boundary layer as well as in the free shear layers [7]. However, it is expected that the introduction of Equation (9) in the one–equation model will result in improved predictions for non–equilibrium turbulent flows [5]; the relation can be recast as

$$\tilde{\epsilon} = f_\mu \sqrt{\tilde{C}_\mu}\eta\, k \tag{10}$$

where $\tilde{\epsilon}$ can be used as a bound on the time scale as

$$T_t = \frac{k}{\max(\epsilon;\, \tilde{\epsilon})} = \frac{k}{\max\left(\epsilon;\, f_\mu \sqrt{\tilde{C}_\mu}\eta\, k\right)} \tag{11}$$

An analogous time scaling bound is used in the v^2–f model to abandon the "stagnation point anomaly" signifying that the eddy–viscosity formulation gives an erroneous normal stress difference [21]. On the other hand, near a wall the flow is not turbulent and hence the use of the dynamic time scale k/ϵ is not appropriate. Employing k/ϵ results in vanishing the time scale when approaching a wall, where $k \to 0$ and ϵ is non–zero. To avoid this, the Kolmogorov time scale $\sqrt{\nu/\epsilon}$ is used as a lower bound, where the viscous dissipation is dominant:

$$T_t = \max\left(\frac{k}{\tilde{\epsilon}};\, C_T\sqrt{\frac{\nu}{\tilde{\epsilon}}}\right), \quad \tilde{\epsilon} = \max\left(\epsilon;\, f_\mu \sqrt{\tilde{C}_\mu}\eta\, k\right) \tag{12}$$

In k–ϵ models, this approach prevents the singularity in the dissipation equation down to the wall. Equation (12) warrants that the eddy time scale never falls below the Kolmogorov time scale $C_T\sqrt{\nu/\epsilon}$, dominant in the immediate

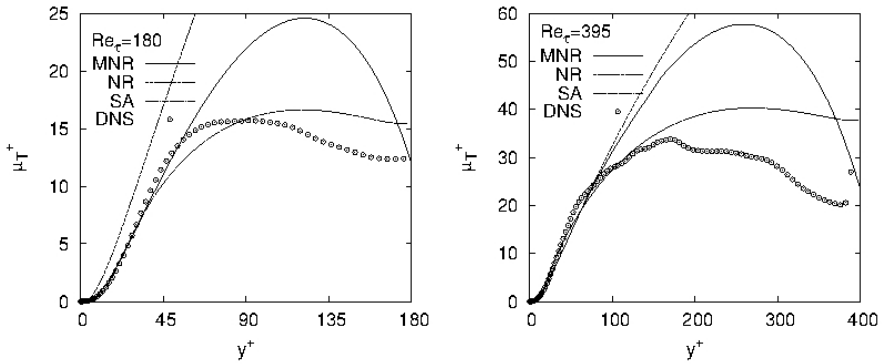

Fig. 6. Turbulent eddy–viscosity profiles of channel flow.

neighborhood of the solid wall. The empirical constant $C_T = \sqrt{2}$ associated with the Kolmogorov time scale is estimated from the behavior of k in the viscous sublayer [22].

The eddy–viscosity damping function f_μ faces the distinct effects of LRN and wall proximity in the near–wall region. Alternatively, the primary objective of introducing f_μ with turbulence models is to represent the kinematic blocking by the wall. The eddy–viscosity damping function included in Equation (5) is chosen pragmatically as

$$f_\mu = tanh\left(\frac{Re_y}{75}\right)\left(1 + \frac{2A_\mu}{Re_y^{3/2}}\right), \qquad A_\mu = \max\left(8;\ \eta T_t\right) \tag{13}$$

A plot of $C_\mu f_\mu$ against the DNS data [13] for fully developed turbulent channel flows is shown in Figure 1, where the abbreviations NR and MNR stand for the models of Norris–Reynolds and modified Norris–Reynolds. A good correlation with the DNS data is obtained for the MNR model. The empirical function f_μ is valid in the whole flow field, including the viscous sublayer and the logarithmic layer. In the region close to the wall, the Reynolds stress $-\overline{uv} \sim y^3$ and $k \sim y^2$. To preserve the correct cubic power–law behavior of $-\overline{uv}$, the damping function (herein the product of $C_\mu f_\mu$) needs to increase proportionally to y^{-1} in the near–wall region. Equation (13) confirms that $C_\mu f_\mu \sim y^{-1}$ in close proximity to the wall. As evinced by Figure 1 in comparison with the DNS data, the adopted form of $C_\mu f_\mu$ reproduces the asymptotic limit involving the distinct effects of LRN and wall proximity. The product of $C_\mu f_\mu \approx 0.09$ (the standard choice for $C_\mu = 0.09$, pertaining to the linear k–ϵ model) remote from the wall to ensure that the model is compatible with the standard k–ϵ turbulence model. The use of Re_y confronts the singularity at neither the separating nor the reattaching point in contrast to the adoption of $y^+ = u_\tau y/\nu$. Consequently, the model is applicable to separated and reattaching flows.

4. Computations

To validate the proposed modifications to the NR model, two cases of one/two–dimensional turbulent flows consisting of a fully developed channel flow and a backward facing step flow are computed. To evaluate the model reliability and accuracy, the MNR model predictions are compared with those from the original NR model and the SA model [4] . However, compared with the NR and SA models, the MNR is additionally sensitized to non–equilibrium and anisotropic effects (i.e., anisotropic model coefficients, depending non–linearly on both the rotational and irrational strains).

A cell centered finite–volume scheme combined with an artificial compressibility approach is employed to solve the flow equations [23–25]. A fully upwinded second–order spatial difference is applied to discretize the convective terms. Roe's damping term [26] is used to calculate the flux on the cell face. A diagonally dominant alternating direction implicit (DDADI) time integration method [27] is applied for the iterative solution of the discretized equations. A multigrid method is utilized for the acceleration of convergence [28]. The basic implementation of the artificial compressibility method and associated features of the computational method are described in References [23–25].

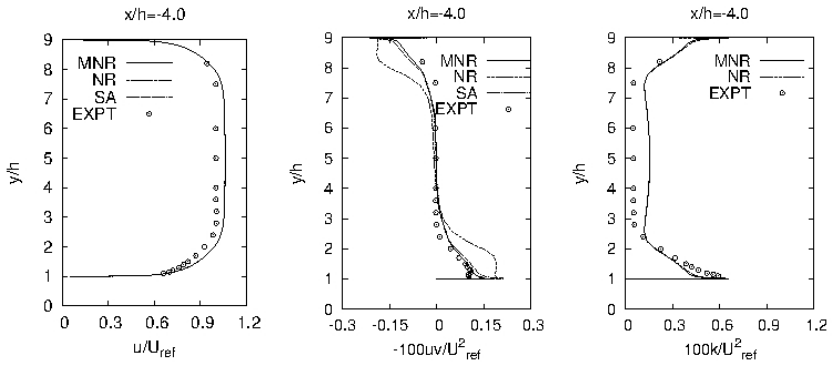

Fig. 7. Inlet profiles for step flow.

A variable grid spacing is used to resolve the sharp gradient in the near–wall regions. Grid densities are varied to ensure the grid independence of the numerical results. In the computations, convergence of the solution is judged by monitoring the root–mean–square residuals of the flow variables. The solution is considered converged when residuals of all flow variables are of the order of 10^{-4} or less.

4.1. Turbulent channel flow

The plane channel is the most common flow utilized to evaluate turbulence models. Computations are performed for fully developed turbulent channel flows at $Re_\tau = 180$ and 395 for which turbulence quantities are available from the DNS data [13] . The calculations are conducted in the half–width of the channel, using a one–dimensional RANS solver. The computation involving a 1×64 non–uniform grid refinement is considered based on the grid independence test. To ensure the resolution of the viscous sublayer the first grid node next to the wall is placed at $y^+ = u_\tau y/\nu \approx 0.3$. Computed results are plotted using the non–dimensional variables $u^+ = u/u_\tau$, $k^+ = k/u_\tau^2$, $\overline{uv}^+ = \overline{uv}/u_\tau^2$ and $\epsilon^+ = \nu\epsilon/u_\tau^4$ versus y^+.

The computation yields an Re_τ within approximately 2% of the DNS value for the MNR and SA models, indicating that the pressure and drag forces are in balance. Figure 2 shows the velocity profiles for different turbulent models. Predictions of the MNR and SA models agree quite well with the DNS data. The NR model appears to under–estimate the mean velocity beyond y^+ of about 10. Profiles of turbulent shear stresses are displayed in Figure 3. Agreement of both the MNR and SA model predictions with the DNS data is fairly good. The NR model follows the DNS data near the wall, but over–predicts $\overline{uv}^+$ beyond the near–wall region. It seems likely that the MNR model returns slightly superior predictions in the near–wall regions relative to the SA model.

Further examination of the model performance is directed to the k^+ profile as portrayed in Figure 4. As is evident, k^+ of the MNR model agrees well with the DNS at least in the near–wall region. The NR model predictions appear to follow the DNS data closely near the wall, however diverges from the DNS data in the buffer and outer layers. Figure 5 exhibits the profile of ϵ^+ from both the NR and MNR computations. The MNR model provides maximum ϵ^+ values near the wall which are more in line with the experimental and DNS data. As is observed, compared with the DNS data the NR model produces excessive ϵ^+ in the buffer layer where y^+ is about 30. Nevertheless, MNR and NR share the characteristic of similar agreement with the DNS data in the outer layer. Figure 6 shows the turbulent eddy–viscosity profiles. As notable from the figure, both the SA and MNR models reproduce the correct near–wall behavior, comparable with the DNS data. However, both model predictions are inaccurate beyond $y^+ = 50$. Surprisingly, this inaccuracy has a little impact on the mean flow and other turbulent parameters since they are reasonably predicted. As can be seen, the NR model greatly over–estimates the turbulent eddy–viscosity beyond the near–wall region. Apparently, the observed discrepancy of NR model with DNS data is due to the fact that its applicability is confined within the wall layer as noted in Reference [2].

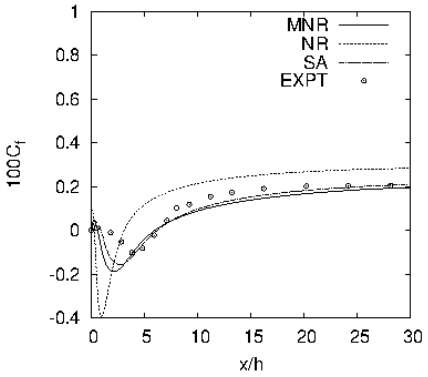

Fig. 8. Skin–friction coefficient along the step–side bottom wall.

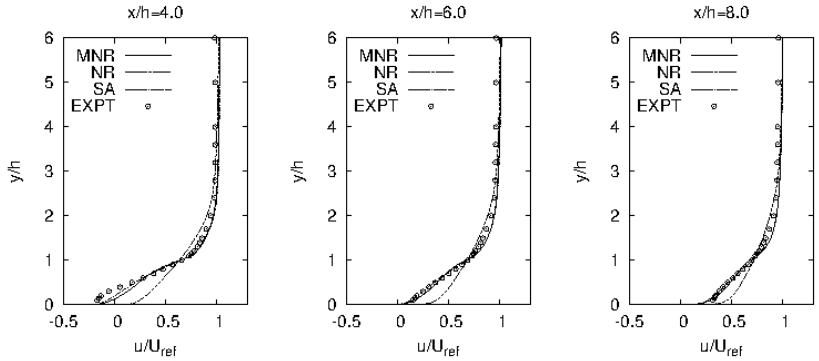

Fig. 9. Mean velocity profiles at selected locations for step flow.

4.2. Backward facing step flow

To validate the performance in complex separated and reattaching turbulent flows, the MNR model is applied to the flow over a backward facing step flow. The computation is conducted corresponding to the experimental case with a zero deflection of the wall opposite to the step as investigated by Driver and Seegmiller [29]. The ratio between the channel height and the step height h is 9, and the step height Reynolds number is $Re = 3.75 \times 10^4$. At the channel inlet, the Reynolds number based on the momentum thickness is $Re_\theta = 5 \times 10^3$. For the computations, grids are arranged in two blocks. The smaller one (extended from the inlet to the step) contains a 16×48 non–uniform grid and the non–uniform grid size for other one is 128×80. The maximum height of the first near–wall grid node is at $y^+ < 1.5$. The distance x/h shown below is measured exactly from the step corner.

The inlet profiles for all dependent variables are generated by solving the models at the appropriate momentum thickness Reynolds number. Profiles of mean velocity, shear stress and turbulent kinetic energy at the inlet are presented in Figure 7. The MNR and SA models ensure close adherence to the experimental data. The NR model predicts the velocity and turbulent kinetic energy profiles that are in a fair agreement with the measurement. However, this model exhibits some discrepancies between the predictions and the data for the shear stress profile, especially in the near–wall region.

Computed and experimental friction coefficients ($C_f = 2u_\tau^2/U_{ref}^2$, where U_{ref} is a reference inlet velocity) along the step side wall are plotted in Figure 8. Comparing the predicted skin–friction coefficient of various models is one component of the critical evaluation of near–wall turbulence models. As is observed, the NR model gives the C_f–distribution with a large overshoot followed by a sudden drop in the immediate vicinity of the recirculation region.

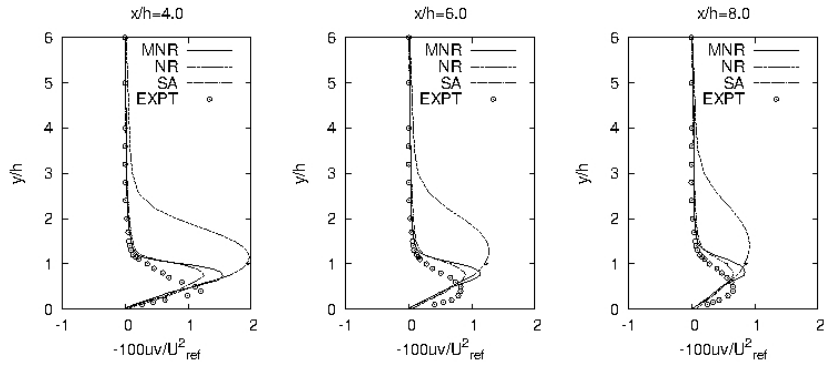

Fig. 10. Shear stress profiles at selected locations for step flow.

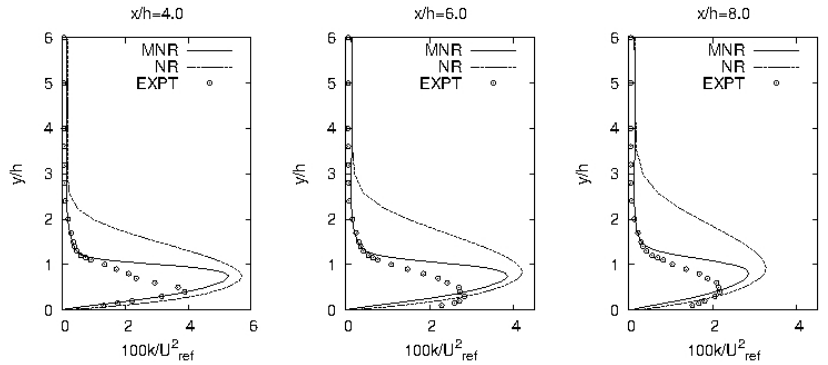

Fig. 11. Kinetic energy profiles at selected locations for step flow.

The positive C_f that starts from $x/h = 0$, is due to a secondary eddy which sits in the corner at the base of the step, inside the main recirculation region. The NR model predicts a recirculation length of 2.75. The corresponding predictions by the SA and MNR models are 5.1 and 5.27, respectively. The experimental value of the reattachment length is 6.26 ± 0.1, making a fairly good correspondence with the MNR and SA models.

The streamwise mean velocity profiles at three representative positions are depicted in Figure 9. Obviously, the predictions of both the MNR and SA models are in a good agreement with the experiment. It is a bit nebulous that the inaccurate prediction of the C_f–distributions especially in the recirculation region by the MNR and SA models has a little effect on the velocity profiles. The NR model disagrees with the experiment particularly in the near–wall region. Comparisons are extended to the distributions of the Reynolds shear stress and the corresponding turbulent kinetic energy at different x/h locations behind the step corner, as shown in Figures 10 and 11, respectively. A closer inspection of the distribution indicates that the MNR model predictions are in a broad agreement with the experimental data. On average, the agreement is good in both the recirculation and recovery regions. On the contrary, the NR model appears to match the experimental data near the wall, however it predicts excessive $-uv$ and k beyond the near–wall boundary. The SA model is able to cope with the experimental data for the shear stress.

5. Conclusions

The MNR model is susceptible to the near–wall and low–Reynolds number effects issuing from the physical requirements. Since the eddy–viscosity formulation depends non–linearly on both the mean strain–rate and vorticity parametrs, the MNR is capable of evaluating the flow cases with separation and reattachment. The performance evalu-

ation dictates that unlike the original NR model, the MNR model can be employed as a single–equation model instead of associating it with the two–layer model of turbulence.

References

[1] Baldwin BS, Lomax H: Thin layer approximation and algebraic model for separated turbulent flows. *AIAA Paper*, 78–257 (1978).
[2] Norris LG, Reynolds WC: Turbulent channel flow with moving wavy boundary. *Report No. FM–10*, Stanford University, Department of Mechanical Engineering, USA (1975).
[3] Baldwin BS, Barth TJ: A one–equation turbulence transport model for high–Reynolds number wall–bounded flows. *NASA TM–102847* (1990).
[4] Spalart PR, Allmaras SR: A one–equation turbulence model for aerodynamic flows. *AIAA Paper No. 92–0439* (1992).
[5] Mender FR: Eddy viscosity transport equations and their relation to the k–ϵ model. *ASME J. Fluids Engng.* 119, 876–884 (1997).
[6] Allegory M: Assessment and modification of one–equation models of turbulence for wall–bounded flows. *ASME J. Fluids Engng.* 129, 921–928 (2007).
[7] Fares E, Sc hröDee W: A general one–equation turbulence model for free shear and wall–bounded flows. *Flow, Turbulence and Combustion* 73, 187–215 (2004).
[8] Nagano Y, Pei CQ, Hatter H: A new low–Reynolds–number one–equation model of turbulence. *Flow, Turbulence and Combustion* 63, 135–151 (1999).
[9] Rahman MM, Siikonen T, Agarwal RK: Improved low Re–number one–equation turbulence model. *AIAA J.* 49, 735–747, 2011.
[10] Rahman MM, Wallin S, Siikonen T: Exploring k and ϵ with R–equation model using elliptic relaxation function. *Flow, Turbulence and Combustion* 89, 121–148 (2012).
[11] Rodi W: Experience with two–layer models combining the k–ϵ model with a one–equation model near the wall. *AI AA Paper No. 91–0216*, presented at the 29Th Aerospace Science Meeting, Reno, Nevada (1991).
[12] Papanicolaou E, Rodi W: Computation of separated–flow transition using a two–layer model of turbulence. *ASME Journal of Turbomachinery* 121, 78–87 (1999).
[13] Mansour NN, Kim J, Moin P: Reynolds–stress and dissipation–rate budgets in a turbulent channel flow. *J. Fluid Mech.* 194, 15–44 (1988).
[14] Rahman MM, Siikonen T: Compound wall treatment with low–Re turbulence model, *Int. J. Number. Meths. Fluids* 68, 706–723 (2012).
[15] Rahman MM, Siikonen T: An eddy viscosity model with near–wall modifications. *Int. J. Numer. Meths. Fluids* 49, 975–997 (2005).
[16] Rahman MM, Siikonen T: An explicit algebraic Reynolds stress model in turbulence. *Int. J. Numer. Meths. Fluids* 52, 1135–1157 (2006).
[17] Rahman MM, Siikonen T: A low–Reynolds number explicit algebraic stress model. *ASME J. Fluids Engineering* 128, 1364–1376 (2006).
[18] Rahman MM, Siikonen T: An eddy viscosity model with elliptic relaxation approach. *Int. J. Heat Fluid Flow* 30, 319-330 (2009).
[19] Andreas EL, Claffery KJ, Jordan RE, Fairall CW, Guest PS, Persson POG, Grachev AA: Evaluations of the von Karman constant in the atmospheric surface layer. *Journal of Fluid Mechanics* 559, 117–149 (2006).
[20] Bradshaw P, Ferris DH, Atwell NP: Calculation of boundary layer development using the turbulent energy equations. *J. Fluid Mech.* 23, 31–64 (1967).
[21] Durban PA: On the k–ϵ stagnation point anomaly. *Int. J. Heat and Fluid Flow* 17, 89–90 (1996).
[22] Rahman MM, Siikonen T: Modifications for an explicit algebraic stress model. *Int. J. Numer. Meths. Fluids* 35(2), 221–245 (2001).
[23] Rahman MM, Rautaheimo P, Siikonen T: Numerical study of turbulent heat transfer from a confined impinging jet using a pseudo–compressibility method. *In Second International Symposium on Turbulence, Heat and Mass transfer*, Delft, The Netherlands, K. Angelic K, Pewters TWX (eds). Delft University Press: Delft, 511–520 (1997).
[24] Rahman MM, Siikonen T: An artificial compressibility method for incompressible flows. *Numer. Heat Transfer, Part B* 40, 391–409 (2001).
[25] Rahman MM, Siikonen T: An artificial compressibility method for viscous incompressible and low Mach number flows. *Int. J. Numer. Meths. Engng.* 75, 1320–1340 (2008).
[26] Roe PL: Approximate Riemann solvers, parameter vectors, and difference schemes. *J. Comput. Physics* 43(2), 357–372 (1981).
[27] Lombard C, Bearding J, Antipathy E, Alger J: Multi–dimensional formulation of CSCM - an upwind flux difference eigenvector split method for the compressible Naiver–Stokes equations. *In 6th AIAA Computational Fluid Dynamics Conference* AIAA Paper 83–1895–CAP, 649–664 (1983).
[28] Jameson A, Yoon S: Multiplied solution of the Euler equations using implicit schemes. *AIAA J.* 24(11), 1737–1743 (1986).
[29] Driver DM, Seegmiller HL: Features of a reattaching turbulent shear layer in divergent channel flow. *AIAA J.* 23(2), 163–171 (1985).